Proceeding of IMECE05:
2005 ASME International Mechanical Engineering Congress and Exposition
November 5-11, 2005, Orlando, Florida USA

IMECE2005-80095

A HYBRID NUMERICAL MODEL FOR SIMULATING ATMOSPHERIC DISPERSION

Xiuling Wang[1, 2] and Darrell W. Pepper[1, 2]

[1]Nevada Center for Advanced Computational Methods, University of Nevada Las Vegas
[2]Department of Mechanical Engineering, University of Nevada Las Vegas

ABSTRACT

A hybrid numerical model for simulating atmospheric contaminant dispersion is developed. The hybrid numerical scheme employs an hp-adaptive finite element method coupled with a Lagrangian particle transport technique to solve the governing equations for atmospheric flow and species transport. A random walk/stochastic approach is used to generate Lagrangian particles that define the contaminant dispersion traces. A coarse mesh using low order shape functions is initially generated. Both the mesh and shape function order are subsequently refined and enriched in those regions where high computational error exist. Compared with fine mesh and high order numerical solutions, the hybrid scheme produces highly accurate solutions with reduced computational cost. A general probability distribution is used in the particle transport module for the random component of motion due to turbulent diffusion. Results depicting contaminant transport and dispersion in the atmosphere are presented. The computational efficiency of the hybrid numerical model is also discussed.

INTRODUCTION

Contaminant dispersion is a serious environmental problem [1]. Analytical solutions for the equations used to describe the advection and diffusion of contaminants in the atmosphere are intractable for most real-world situations. Consequently, researchers have had to rely upon numerical simulations for many years [2]-[5]. Regardless of which numerical methods researchers may use, the goal has been essentially to achieve fast and accurate predictions of wind fields and contaminant dispersion traces.

The finite element method (FEM), with its ability to easily deal with irregular geometries while employing the use of general-purpose algorithms, is one of the most popular numerical tools for solving contaminant dispersion problems. Adaptive FEM is especially attractive for it can obtain highly accurate results beginning with a coarse mesh and low order shape functions.

In this study, an hp-adaptive FEM is employed to efficiently construct highly accurate 3-D wind fields; a Lagrangian Particle Transport (LPT) technique is coupled to the FEM model. The LPT scheme uses a large number of particles to approximate advection and diffusion - instead of solving the transport equation for species concentration directly.

A brief discussion of the principles describing the two major numerical schemes is presented. Simulation test cases are given for contaminant dispersion released into the atmosphere and enveloping a series of buildings. The simulation is further enhanced as the contaminant enters a window within a building complex and disperses within a set of interior offices.

The hybrid numerical model appears well suited for solving contaminant dispersion related environmental problems. The model can be effective for use in emergency response and homeland security situations.

NOMENCLATURE

B	Body force
C	Gradient operator
D	Domain
∂D	Domain boundary
F_V	Load vector for velocity
F_θ	Load vector for temperature
F_{C_m}	Load vector for mass concentration
h	Characteristic of element length
h_e	Element size
k_h	Horizontal diffusion coefficient
k_z	Vertical diffusion coefficient
k_e	Streamline component of the diffusion tensor
L	Linear operator
M	Mass matrix
N_i	Shape function

n	Previous time level
n+1	New time level
p	Shape function order
P	Pressure
t	Time
V	Velocity vector
V^*	Perturbed velocity vector
x	Space
z	Random displacement associated with dispersion
α	Petrov-Galerkin coefficient
β	Cell Peclet numbe
θ	Temperature
ω	Angular velocity of the earth
ψ	Latitude
C_m	Species concentration
g	The acceleration of gravity
Q	The radiative cooling / heating of the atmosphere
S_{C_m}	The source/sink term

GOVERNING EQUATIONS

The governing equations that describe three-dimensional atmospheric flow and species transport can be written as:

Conservation of Mass:

$$\frac{\partial \rho}{\partial t}+\frac{\partial \rho u}{\partial x}+\frac{\partial \rho v}{\partial y}+\frac{\partial \rho w}{\partial z}=0 \tag{1}$$

Conservation of Momentum:

X-direction:

$$\frac{\partial \rho u}{\partial t}+\frac{\partial \rho u^2}{\partial x}+\frac{\partial \rho uv}{\partial y}+\frac{\partial \rho uw}{\partial z}=\frac{\partial}{\partial x}\left(k_h\frac{\partial u}{\partial x}\right)+\frac{\partial}{\partial x}\left(k_h\frac{\partial u}{\partial x}\right)+\frac{\partial}{\partial x}\left(k_z\frac{\partial u}{\partial x}\right)+2v\omega\sin\psi-2w\omega\sin\psi-\frac{\partial p}{\partial x} \tag{2}$$

Y-direction:

$$\frac{\partial \rho v}{\partial t}+\frac{\partial \rho uv}{\partial x}+\frac{\partial \rho v^2}{\partial y}+\frac{\partial \rho vw}{\partial z}=\frac{\partial}{\partial x}\left(k_h\frac{\partial v}{\partial x}\right)+\frac{\partial}{\partial y}\left(k_h\frac{\partial v}{\partial y}\right)+\frac{\partial}{\partial z}\left(k_z\frac{\partial v}{\partial z}\right)+2u\omega\sin\psi-\frac{\partial p}{\partial y} \tag{3}$$

Z-direction:

$$\frac{\partial \rho w}{\partial t}+\frac{\partial \rho uw}{\partial x}+\frac{\partial \rho vw}{\partial y}+\frac{\partial \rho w^2}{\partial z}=\frac{\partial}{\partial x}\left(k_h\frac{\partial w}{\partial x}\right)+\frac{\partial}{\partial y}\left(k_h\frac{\partial w}{\partial x}\right)+\frac{\partial}{\partial z}\left(k_z\frac{\partial w}{\partial z}\right)-g-\frac{\partial p}{\partial z} \tag{4}$$

Conservation of Energy:

$$\frac{\partial \theta}{\partial t}+\frac{\partial u\theta}{\partial x}+\frac{\partial v\theta}{\partial y}+\frac{\partial w\theta}{\partial z}=\frac{\partial}{\partial x}\left(k_h\frac{\partial \theta}{\partial x}\right)+\frac{\partial}{\partial y}\left(k_h\frac{\partial \theta}{\partial y}\right)+\frac{\partial}{\partial z}\left(k_z^{\theta}\frac{\partial \theta}{\partial z}\right)+Q \tag{5}$$

Species Transport:

$$\frac{\partial C_m}{\partial t}+\frac{\partial uC_m}{\partial x}+\frac{\partial vC_m}{\partial y}+\frac{\partial wC_m}{\partial z}=\frac{\partial}{\partial x}\left(k_h\frac{\partial C_m}{\partial x}\right)+\frac{\partial}{\partial y}\left(k_h\frac{\partial C_m}{\partial y}\right)+\frac{\partial}{\partial z}\left(k_z^{\theta}\frac{\partial C_m}{\partial z}\right)+S_{C_m} \tag{6}$$

where K depicts the exchange coefficients for diffusion $K \equiv k_h\vec{i}+k_h\vec{j}+k_z\vec{k}$; C_m is the species concentration; g is the acceleration of gravity; Q is the radiative cooling/heating of the atmosphere; S_{C_m} is the source/sink term which includes changes of state, chemical transformations, precipitation, and sedimentation.

The modeling of turbulence and resulting forms of closure are quite varied. Examples of turbulence closure schemes involving first and second order terms are discussed by Pielke [6]. In this study, a simple gradient diffusion approach is first employed; horizontal mixing is approximated using the relation proposed by Smagorinsky et al [7], e.g., the intensity of horizontal mixing is related to the strength of the horizontal wind shear

$$k_h=\frac{1}{2}k_o^2h_e^2\left[\left(\frac{\partial u}{\partial x}-\frac{\partial v}{\partial y}\right)^2+\left(\frac{\partial v}{\partial x}+\frac{\partial u}{\partial y}\right)^2\right]^{\frac{1}{2}} \tag{7}$$

where h_e is the average element length and k_o is von Karman's constant. The vertical exchange coefficients of momentum, heat, and moisture are given in the surface layer by the relations see Businger et al [8]; Blackadar [9], Monin and Yaglom, 1971 [10].

$$k_z=\frac{k_o u^* z}{\phi_m(\zeta)} \quad k_z^{\theta}=k_z^{q}=\frac{k_o u^* z}{\phi_H(\zeta)} \tag{8}$$

where ϕ_H (ς) is the mean vertical temperature profile of the surface layer. Above the surface layer, the exchange coefficients are defined according to McNider and Pielke [11].

An objective analysis technology is employed to construct a diagnostic mass-consistent initial wind field before solving the prognostic equations of atmospheric motion. Surface wind fields are first constructed from meteorological tower data using interpolation onto the initial mesh with inverse distance-squared weighting [12]. Upper level winds are subsequently interpolated to establish an initial 3-D wind field. An Euler-Lagrange variational formulation is solved for the potential and the velocities corrected to ensure mass consistency.

The diagnostic wind field is used as input for the prognostic solution. Instead of initializing with zero values for winds, the diagnostic procedure produces a realistic approximation to the overall wind field.

FINITE ELEMENT FORMULATION

Trilinear hexahedral elements are used to discretize the problem domains. The Galerkin weighted residual method is employed for Eqs (1-6). The corresponding matrix equivalent forms for the resulting integral expressions can be expressed as:

$$C^T\{V\}=0 \tag{9}$$

$$[M]\{\dot{V}\}+([K]+[A(V)])\{V\}+C^T\{p\}=\{F_V\} \tag{10}$$

$$[M]\{\dot{\theta}\}+([K_\theta]+[A(V)])\{\theta\}=\{F_\theta\} \tag{11}$$

$$[M]\{\dot{C}_m\} + ([K_m] + [A(V)])\{C_m\} = \{F_{C_m}\} \quad (12)$$

where $[M]$ is the mass matrix, $[K]$ is the diffusion matrix, $[A(V)]$ is the advection matrix and C^T is the gradient operator. For detailed matrix coefficients definition see Pepper and Stephenson [13].

The advection terms are weighted by Petrov-Galerkin Scheme:

$$W_i = N_i + \frac{\alpha h_e}{2|V|}\left[V \cdot \nabla N_i\right] \quad (13)$$

$$\alpha = \coth\beta - \frac{1}{\beta}, \beta = \frac{|V| h_e}{2K_e} \quad (14)$$

where K_e is the streamline component of diffusion tensor.

Mass lumping is used in order to obtain a fully explicit time scheme. Mass matrix is diagonalized or lumped. The inverse of the mass matrix becomes:

$$[M]^{-1} = \frac{1}{m_i} \quad (15)$$

HP-ADAPTIVE FINITE ELEMENT METHODOLOGY

Generally, there are four main categories of adaptation: h-adaptation, where the element size varies while the order of shape function remains constant; p-adaptation, where the element size is constant while the order of the shape function is increased to meet the desired accuracy requirement; r-adaptation, where spring analogy redistributes the nodes in an existing mesh; and hp-adaptation, which is the combination of both h-and p-adaptation. Among these four basic schemes, hp-adaptation is the most promising as it can produce highly accurate results with significantly less computational cost. It has been demonstrated that hp-adaptive FEM is one of the best mesh-based schemes [14]. The application of h-adaptive FEM has seen limited use in literature for solving environmental transport problems [13] [15]. To the best of our knowledge, no one has reported the use of hp-adaptive FEM for solving atmospheric contaminant dispersion in the existing literature.

Specific adaptation rules must be followed in order to guarantee adaptive process can be carried on successfully. Adaptation is a complex procedure; only the most important rules for h-adaptation, p-adaptation and hp-adaptation are briefly stated in the following sub-sessions.

h-adaptation rules

Unstructured anisotropic mesh is allowed which is an efficient, directional refined mesh where refinement in one directional is needed; the I-Irregular mesh refinement rule allows an element to be refined only if its neighbors are at the same or higher level (I-Irregular mesh), by following this rule, multiple constrained nodes (parent node themselves are constraint nodes) can be avoided.

p-adaptation rules

For hierarchical shape functions employed in p-adaptation, they can be categorized as: node functions, edge functions, face functions (for 3D cases) and bubble functions. The minimum rule states that the order for an edge common for two elements never exceeds orders of the neighboring middle nodes. For rectangular elements in 2D cases, both the horizontal and vertical order is considered.

hp-adaptation rules

As a combination of h- and p-adaptation, hp-adaptation can be either refined (unrefined) or enriched (unenriched) whenever necessary. The adaptation rules for h- and p- carry out to and combine together in hp-adaptation. Besides those, to maintain continuity of global basis function, constraints at the interface of elements supporting edge functions of different order are employed. A generalization of the hp-constraints is introduced by Demkowicz et al [16].

Adaptation Algorithm

The hp-adaptive strategy employed in this study is similar to the "three-step hp adaptive strategy" developed by Oden et al [17]. A sequence of refinement steps is employed. Three consecutive hp adaptive meshes are constructed for solving the system equations in order to reach a preset target error: initial coarse mesh, the intermediate h-adaptive mesh, and the final hp adaptive mesh obtained by applying p adaptive enrichments on the intermediate mesh. The p-adaptation is carried out when the problem solution is pre-asymptotic. The whole procedure can be described briefly as follows:

1. Generate an initial coarse mesh
2. Compute problem solution based on current mesh
3. Compute the energy norm of the difference between the current solution and the fine mesh solution
4. If (error is less then preset error tolerance) then
   post process the solution
   else
   If the computational result is not pre-asympotic, then
   adaptively refine the mesh (h-adaptation)
   goto step 2
   else
   adaptively enrich the mesh (p-adaptation)
   goto step 2
   End if
   End if

LAGRANGIAN PARTICLE TRANSPORT

Generally, three main categories exist for dealing with the advection-dispersion contaminant transport problems. They are Eulerian Methods; Lagrangian Methods; and Mixed Eulerian-Lagrangian Methods, which are described in detail by Zheng and Bennett [18].

In this study, one of the Lagrangian methods: a Random Walk Advective and Dispersive Model (RADM) is used to predict contaminant transport trajectories.

This method, followed by the early work of Runchal [19], solves the transport equation for species concentration through a large number of particles, each of which is advected according to the equation:

$$x_t - x_0 = \int_{t_0}^{t} U(x_t, t')dt' + \int_{t_0}^{t} D(x_t, t')dw_{t'} \quad (16)$$

where x_0 the initial condition, U is a mean velocity vector defined over a suitable time interval, and D is a deterministic forcing function for the random component of motion.

Eq. (16) can be further simplified to:

$$\delta x(w,t) = \delta x_U + \delta x_D \quad (17)$$

where the stochastic integral is written as:

$$\delta x_D(w,t) = \int_{t_0}^{t} n_r \sqrt{2K}\, dt' \quad (18)$$

In this instance, $\frac{D^2}{2}$ is assumed to be equivalent to K, and n_r is a normally distributed random number with a mean value of zero and a standard deviation of unity.

For further simplification, Eq. (18) can be written as:

$$\delta x_D = n_r \sigma \quad (19)$$

$$\sigma^2 = \int_{t_0}^{t} 2K dt' \quad (20)$$

Finally the displacement, Eq.16, can be expressed as:

$$x_t - x_0 = \int_{t_0}^{t} U(x_{t'}, t')dt' + n_r \left(\int_{t_0}^{t} 2K(x_{t'}, t')dt'\right)^{1/2} \quad (21)$$

For a rigorous application of the random walk method, the net particle displacement must be calculated by integration of Eq. (21). However, U and K are arbitrary functions of space and time, and it is not always possible to obtain a closed form solution to this equation. For suitably small time steps, it often proves adequate to assume that the mean velocity and the random components can be separately calculated and linearly superimposed.

In the application of RADM, velocity fields are constructed accurately by using the hp-adaptive finite element model; the random component of motion due to dispersion is calculated from a general probability distribution or correlation function.

The calculation to advance the particle in time proceeds in steps as described as follows:

$$x_i(t + \Delta t) = x_i(t) + U_i \Delta t \quad (22)$$

The velocity components are the fictitious total velocities determined for the beginning of the time interval and initial particle positions. Every particle is advanced each time step using Eq. (22). Thus the particle traces out in time a trajectory for the pollutant material.

SIMULATION RESULTS

Problem definition

Air distribution patterns and pathways of contaminant dispersion around building areas are simulated in this study. The configuration for the buildings is shown in Fig.1. Several buildings with different height are displayed within the area.

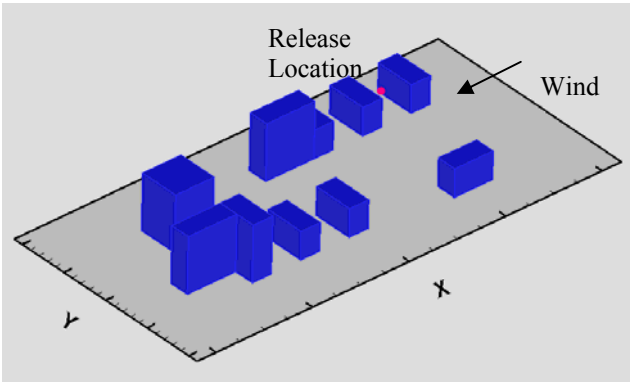

Figure 1: Buildings layout and flow direction

A contaminant release is hypothetically placed near one of the buildings (denoted by the circular dot between the upper right two buildings). The wind flow direction is from right to left, as shown by the arrow in Fig. 1.

Computational mesh

Figure 2 shows the initial computational mesh. The coarse mesh consists of 9345 nodes and 7626 elements.

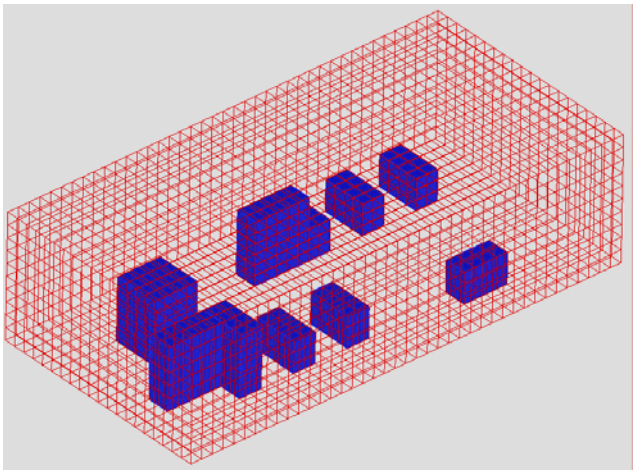

Figure 2: Initial computational mesh

The intermediate mesh is shown in Fig. 3. H-adaptation has been employed to produce the intermediate mesh, which contains 18399 elements and 25476 nodes. Notice that the elements become refined in various regions adjacent to the buildings. A 3-level, h-adaptation has been reached.

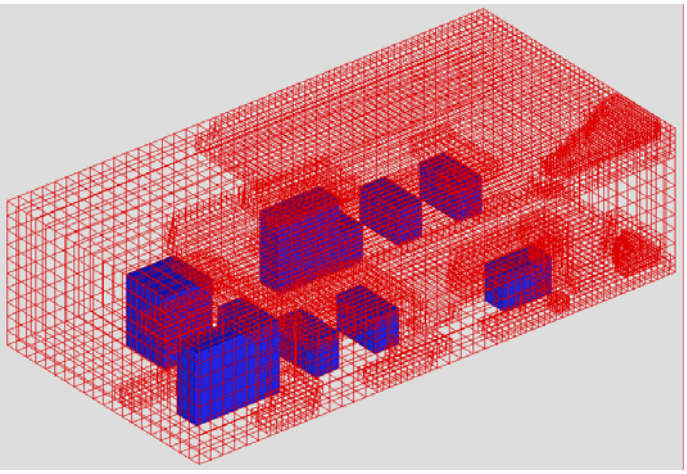

Figure 3: Intermediate h-adaptive mesh

Figure 4 shows the final mesh. The final mesh is obtained when p-adaptation has been employed on the intermediate h-adaptive mesh. The final hp-adaptive mesh consists of 25589 nodes and 18399 elements with 45651 DOF. In this sequence, higher order shape functions have been employed in those regions where the elements are clustered. This is to be expected from the preliminary results observed in the intermediate mesh. Third order p-adaptation has been reached.

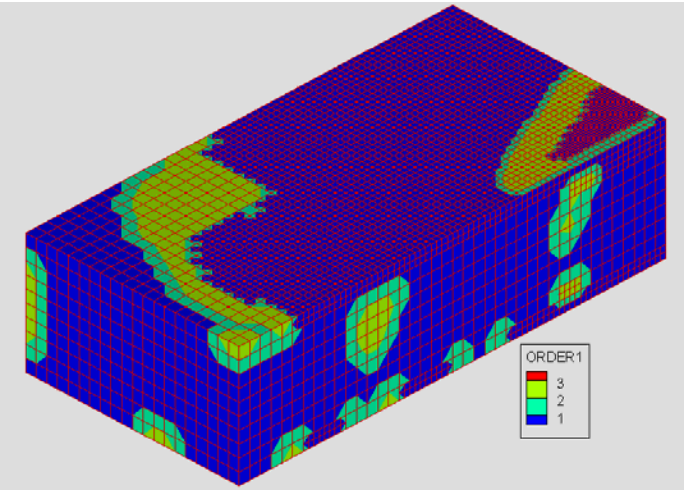

Figure 4: Final hp-adaptive mesh

Following the application of the hp-adaptive FEM sequence, the wind fields are then constructed. The wind vector distributions around the buildings are depicted in a horizontal slice and a vertical slice as shown in Figs. 5 and 6, respectively. Notice the recirculation regions between neighboring buildings in both the horizontal and vertical slices.

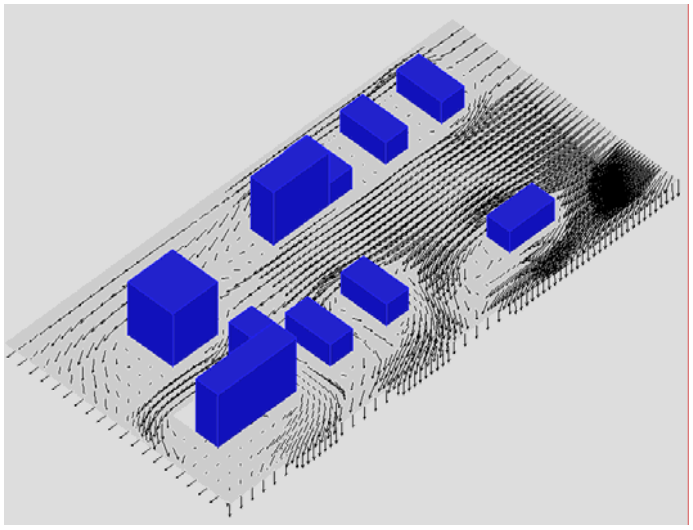

Figure 5: Velocity vectors in horizontal slice

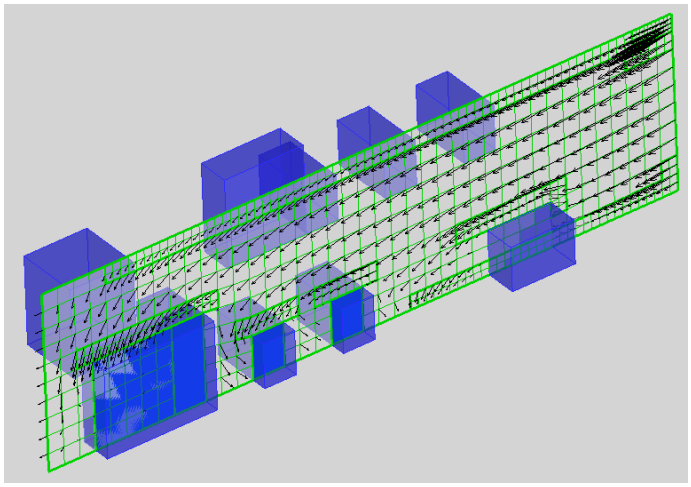

Figure 6: Velocity vectors in vertical slice

Employing the LPT module, a series of contaminant transport traces are depicted in Fig. 7. The different colors of the particles denote particles with different physical properties, e.g., less dense and more dense particles (with gravitational settling). By using LPT technology, the contaminant dispersion traces can be easily visualized, providing visual information for people to avoid those regions with high contaminant concentrations.

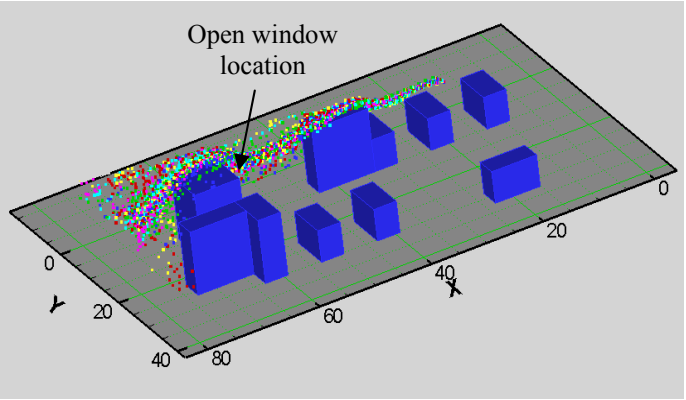

Figure 7: Contaminant dispersion traces

One of the windows in the set of office buildings is assumed to be open (Fig. 7), allowing the contaminant to enter the building. The contaminant (particles) flow inside the office complex, and disperse within the room.

A suite of offices adjacent to a hallway is shown in Fig. 8. The configuration of the office complex consists of three rooms with separate doors and windows. Each office contains a table, a desk, and an office chair.

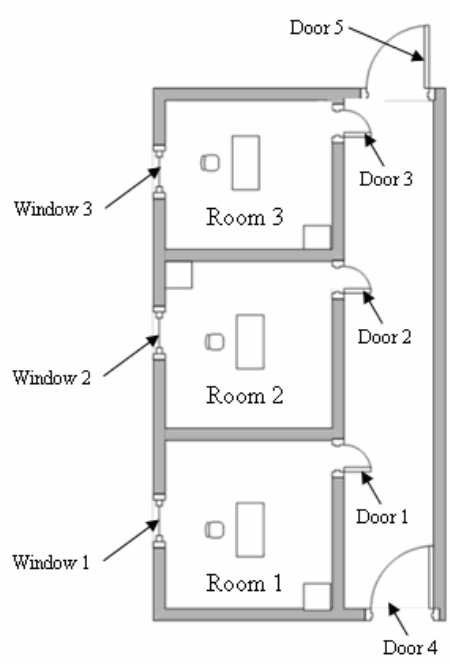

Figure 8: 2-D office complex configuration

Ventilation air is assumed to flow into the hallway through door 4; window 1 is assumed to be open. All the other doors are open with windows 2 and 3 closed. The contaminant material enters the office complex through window 1. The contaminant dispersion traces within the office complex are shown in Fig. 9.

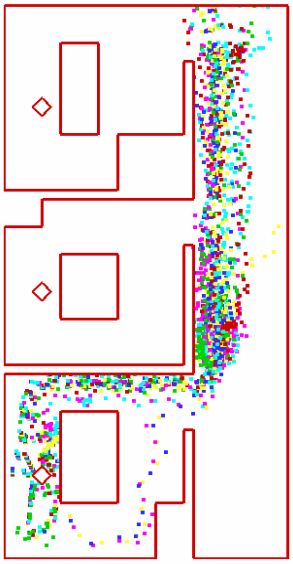

Figure 9 Contaminant dispersion traces with office complex

From Fig. 9 we can see that, since window 1 is open, the contaminant material enters room 1 and becomes dispersed around the desk. Rooms 2 and 3 are essentially contaminant free regions (since both windows are closed) with the air in offices 2 and 3 being relatively stagnant. Because interior air flows in through door 4, the lower part of the hallway is almost contaminant free. It is especially important for inhabitants to be aware of the contaminant dispersion – contaminated regions should be avoided where high contaminant concentrations exist (as down the hallway).

Computational Comparisons

In order to examine the computational efficiency of the hp-adaptive FEM, comparisons are made between the computational times and iteration requirements associated with the adaptive algorithm and a uniformly refined/enriched fine mesh employing a high order FEM algorithm.

The comparison case relates to the interior contaminant dispersion problem previously described [20]. Computational times are compared between the fine mesh/higher order FEM solution and the hp-adaptive FEM solution in constructing steady-state velocity fields within the office complex.

The initial computational mesh is shown in Fig. 10, which consists of 389 quadrilateral elements and 500 nodes.

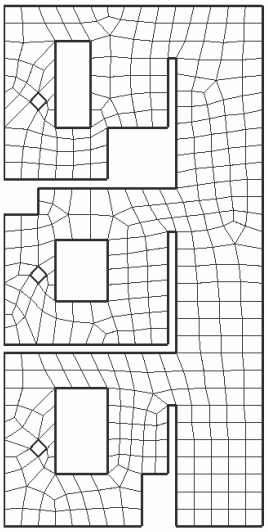

Figure 10: Initial mesh for 2-D office complex

The final computational mesh is shown in Fig. 11, which contains 530 elements with 1374 total degrees of freedom (DOF). Fourth level h- and p- adaptation have been reached.

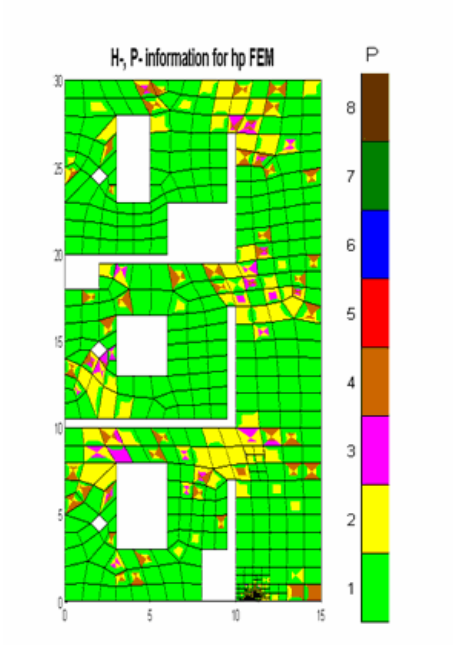

Figure 11: Final mesh for 2-D office complex

A comparison of results is shown in Table 1. To reach the same error criteria $\varepsilon \leq 10^{-5}$, the hp-adaptive algorithm (h = 4, p = 4) is almost 3 times faster than the non-adaptive algorithm (h = 2, p = 2).

Since the 4th order h-p requires considerable CPU time, a 2nd order h-p adaptation was used for comparison.

Table 1.Performances compare for different algorithms

Comparisons		Uniform h (2 levels) and p (2nd order)	Hp-adaptive FEM (h,p-4 levels)
No. of Elements	Initial	1556	389
	Final	1556	530
DOF	Initial	6683	6683
	Final	500	1374
CPU Time (sec)		107388	31080
CPU/DOF (sec/DOF)		16.07	22.62
Iterations		17535	16509

CONCLUSION AND FUTURE WORK

In this paper atmospheric wind fields are constructed using an hp-adaptive finite element method. Contaminant transport traces are simulated using Lagrangian particles that are advected and diffused based upon the velocity fields obtained from the FEM module. The hp-adaptive FEM permits an accurate flow field to be constructed. The LPT scheme permits contaminant transport traces to be quickly simulated. Compared with uniformly refined and enriched FEM, the hp-adaptive FEM is more computational efficient. The numerical scheme is effective in simulating wind fields and contaminant transport around buildings, as well as providing valuable information for risk assessment associated with dispersion of hazardous materials. The method is especially appealing for simulating the intrusion of contaminants into buildings and dispersion within building interiors.

ACKNOWLEDGMENTS

Financial support from the US Department of Energy (DOE) is greatly appreciated.

REFERENCES

[1] Meroney, R. N., "Perspectives on air pollution aerodynamics", 10th International Wind Engineering Conference, Copenhagen, Denmark, 1999.

[2] Nielsen, P. V.," Flow in air conditioned room," PhD Thesis, Tech. Univ. of Denmark, 1974.

[3] Hjertager, B. H. and Magnussen, B. F., "Numerical Prediction of three dimensional turbulent buoyant flow in a ventilated room," Heat Transfer and Turbulent Buoyant Convection, Vol.2, Hemisphere, Washington, DC, pp.429-441., 1977.

[4] Awbi, H. B., "Application of computational fluid dynamics in room ventilation," Build. Environ. 24, pp. 73-84., 1989.

[5] Murakam, S., Kato, S., and Suyama, Y., "Three-dimensional numerical simulation of turbulent airflow in a

ventilated room by means of a two equation model," ASHRAE Trans., 93(2), pp. 621-642., 1987.
[6] Pielke, R. A., "Mesoscale Meteorological Modeling", Academic Press, Orlando, FL, 612 p., 1984.
[7] Smagorinsky, J., Manabe, S., and Holloway, Jr., J. L. "Numerical Results from a Nine-Level General Circulation Model of the Atmosphere", Mon. Wea. Rev., 93, pp727-798, 1965.
[8] Businger, J. A., Wyngaard, J. C., Izumi, Y., and Bradley, E. F. , "Flux-profile Relationships in the Atmospheric Surface Layer", J. Atmos. Sci., 28, 181-189, 1971.
[9] Blackadar, A. K., "Gordon and Breach", Advances in Environ. and Sci. Eng., 1, pp50-85, 1979.
[10] Monin, A. S. and Yaglom, A. M., "Statistical Fluid Mechanics: Mechanics of Turbulence", MIT Press, Cambridge, MA, 769 p., 1971.
[11] McNider, R. T. and Pielke, R. A., "Diurnal Boundary-layer Development over Sloping Terrain", J. Atmos. Sci., 38, pp2198-2212., 1981.
[12] Pepper, D. W. and Kern, C. D.,1st. Conf. on Reg. and Meso. Modeling, Anal., and Prediction, Las Vegas, NV, May 6-9., 1976.
[13] Pepper, D. W. and Stephenson, D. E., "An adaptive finite element model for calculating subsurface transport of contaminant", Ground Water, 33, pp.486-496, 1995.
[14] Demkowicz, L., Rachowicz, W., and Devloo, Ph.**,** "A Fully Automatic hp-Adaptivity", Journal of Scientific Computing, Vol 17, Nos. 1-4, December, 2002.
[15] Pepper, D. W. and Carringtoon, D. B., "Application of h-adaptation for environmental fluid flow and species transport", Int. J. Num. Meth. Fluids, vol 31, pp. 275-283, 1999.
[16] Rachowicz, W, Oden, J., Demkowicz, L, "Toward a universal h-p adaptive finite element strategy, part 3. A study of the design of h-p meshes", *Comput. Meth. Appl. Mech. Eng.* 77, pp181-212.
[17] Oden, J. T., Wu, W., and Ainsworth, M.**,** "Three-Step H-P Adaptive Strategy for the Incompressible Navier-Stokes Equations", Modeling, Mesh Generation, and Adaptive Numerical Methods for Partial Differential Equations, Springer-Verlag, pp.347-366, 1995.
[18] Zheng, C-M. and Bennett, G. D., "Applied contaminant transport modeling", 2nd Ed., John Wiley & Sons, Inc., 2002.
[19] Runchal, A. K., "A Random Walk Atmospheric Dispersion Model for Complex Terrain and Meteorological Conditions", presented at the 2nd AMS Joint Conf. Of Air Pollution Metror. March 24-27, New Orlean, LA., 1980.
[20] Wang, X. L and Pepper, D. W., "A cost-effective model for indoor contaminant simulation", 3rd Dubrovnik conference on sustainable development of energy, water and environment systems, June 5-10, Dubrovnik, Croatia, 2005.